

# PRELIMINARY FIELD EVALUATION OF A KA-BAND DOPPLER RADAR FOR FOG AND CLOUD OBSERVATIONS

Kyosuke Hamazu\*<sup>1,2</sup>, Toshio Wakayama<sup>1</sup>, Hiroyuki Hashiguchi<sup>2</sup>,  
Tomoya Matsuda<sup>1</sup> and Shoichiro Fukao<sup>2</sup>

1. Mitsubishi Electric Corporation, Chiyoda-ku, Tokyo, Japan

2. Kyoto University, Uji, Kyoto, Japan

## 1. INTRODUCTION

A Ka-band pulse Doppler radar with a digital phase compensation processor is presented. A radar which uses millimeter wave like Ka-band is very useful for cloud and fog observations as reported by Pasqualucci (1984) and Kropfli et al.(1995). However it is generally difficult to generate high coherent transmitted power, so scanning observations for cloud and fog by a Doppler radar had not been done in the wide range of 20-30 km. We have developed a new Ka-band scan radar, which provides very good Doppler information by using a magnetron for transmitter and a phase compensation processor for random phase shift correction of transmitted pulses.

Since several antenna scan modes, such as PPI, CAPPI, and RHI, are available, optimum mode associated with meteorological environment is selectable.

## 2. SYSTEM CONFIGURATION AND ITS OPERATION

Main specifications of this radar are shown in Table1.

---

\*Corresponding author address : Kyosuke Hamazu, Mitsubishi Electric Corporation, 2-2-3 Marunouchi Chiyoda-ku Tokyo 100-8310, Japan; e-mail : kyosuke.hamazu@hq.melco.co.jp

Transmitted signal with random initial phase output from magnetron is radiated from the antenna to the air and at the same time a part of that diverted signal is recorded for phase correction in the signal processor by way of the receiver. In this signal processor, phase correction is performed to the received echo at every 125m in real-time. Doppler velocity and Doppler spectra are calculated by PPP or FFT based on received phase signal after phase correction with transmitted signal mentioned before and they are output to EWS via SCSI bus. Quick look screen display and data accumulation for later analysis is available in EWS. The system block diagram is shown in Figure 1.

Antenna scanning and other setting are carried out in the above EWS. There are following seven kinds of operational modes, PPI, CAPPI, RHI, POSITION, SECTOR, SPPI, SRHI. Selecting operational mode and setting AZ/EL scanning range are done on EWS screen.

We verified the function of Doppler measurement of this radar by comparing the Doppler velocity obtained by this radar with the neighboring MU radar. Figure 2 shows the example of height profile obtained by MU radar and this radar. Horizontal wind of Doppler velocity was calculated by VAD method. The result confirms the followings: Doppler measurement and velocity unfolding correction algorithm function properly in this

radar since the results of two radars gave good agreement in the velocity more than 30m/s in the range above 1.5km altitude, which is MU radar's observable range.

According to the result of initial observation at the Shigaraki MU observatory, unfolding correction expands the velocity range 4 times as Nyquist velocity Doppler which confirms that Doppler velocity measurement until approx.  $\pm 40\text{m/s}$  is available.

We initially developed the radar as a fixed site model. And then, from the point of the view of convenient observation, a movable one with the same features is developed.

### 3. CLOUD OBSERVATION

Figure 3 shows observation results of multi-layer clouds, which became feeble precipitation close to the ground on the September 17<sup>th</sup>, 1997. Figure 4 shows radar reflectivity factor and vertical velocity obtained by the radar around the same time period. Positive sign of Doppler velocity suggests the direction falling to the ground.

According to Figure 4 (a), there is an area at 2km ~ 4.5km altitude where vertical velocity is beyond 6m/s. It is roughly presumed that area where vertical velocity is large is precipitation and the one where it is small is ice crystal area. It shows that falling speed in this observation sample is roughly divided into three layers according to the vertical profile of falling speed. The first layer is between the ground level and 2km altitude and it's vertical velocity is about +4m/s. In the second layer between 2~4.5km altitude has approximately +6m/s vertical velocity. The third one is above 4.5km altitude where vertical velocity dramatically drops below 1m/s between 4~5km altitude. Especially beyond 6km altitude to 7.5km, the top of clouds, falling speed goes down to 0m/s or minus. Corresponding to the result of radar reflectivity factor measured at the same time

shown in the same figure, we see that very small cloud(ice crystal) in the early stage of generation is formed in the top of the third layer. The top of the cloud is slightly going up, which means that it is growing.

Move on to Figure 4(b) observed 8 minutes later, where the height profile of radar reflectivity factor shows that the border between the second layer and the first layer which was so obvious in Figure 4(a) cannot clearly be distinguished. Maximum point of radar reflectivity factor is in 1~2km altitude while it was in 3~4 km altitude in (a). In the case of vertical velocity as well, maximum point of falling speed goes down close to the ground. Moreover echo top stops developing as ice crystal tends to fall. The same tendency is seen in Figure 4(c) observed 4 minutes later, where both maximum radar reflectivity factor and maximum falling speed move down to the lower altitude than in (b). This series of observation results indicate that precipitation particles which keep evaporating until falling down close to the ground reach the earth and soon it starts raining.

Figure 5(a) shows the sample of double-structure cloud observed on July 17<sup>th</sup>, 1997. In the RHI observation of radar reflectivity factor in the same figure, double-structure cloud is clearly detected where there are the first layer with 500m thickness around 6km altitude and the second layer with 1500m thickness near 8km altitude.

Figure 5(b) shows the sample of cumulonimbus cloud observed on August 6<sup>th</sup>, 1997. Diameter of the lower part is about 6km and the cloud top reaches 10km. This is a growing cumulonimbus cloud whose cloud top develops from 6km to 10km in approximately 5minutes according to the 20 seconds interval RHI observation.

In this way, it is confirmed that structure and developing process of clouds are observed in details by the Ka-band Doppler radar.

#### 4. FOG OBSERVATION

There are annually a number of foggy days in eastern Pacific coast of Hokkaido and the offshore. Especially in July and August it is sometimes covered with fog all day long. Hence, ocean fog observation was often performed in 1980's mainly in Kushiro district. Yanagisawa et al.(1986) discussed about relation between radar reflectivity factor and particle diameter distribution of fog, radar echo type, etc. On the other hand, as Doppler observation and three dimensional observation of horizontal/vertical section distribution of fog were not performed due to the limitation of the radar at that time, the three dimensional structure and moving mechanism were expected to be clarified. We set this radar (mobile model) at the Kushiro airport in July and August, 1999 and performed initial observation.

Figure 6 shows the location of this airport and the observation area. Figure 7 shows observation view of this radar.

The fog occurred the night before remained until 10:00 on August 5<sup>th</sup>, 1999. Figure 8 is the sample of PPI screen obtained after the meteorological observation started. In this figure, the range is 10km radius.

Figure 9(a) and (b) show RHI screens observed toward the ocean at AZ 180° that is the same echo as shown in Figure 8. Figure 9(a) indicates radar reflectivity factor and (b) indicates Doppler velocity. Radar reflectivity factor distribution in (a) shows a constant echo top pattern typical for fog and a wave-shape structure rising from the south to the north is also admitted. Here take a look at the vertical section of Doppler velocity in (b), where Doppler velocity changes discontinuously at the border of 300m altitude in the high-level layer and the low-level layer. That is, Doppler velocity in the low-level layer is approximately 0m/s and in the high-level layer, where Doppler velocity is coming

toward the radar; to the north, is 4~6m/s as it is clearly shown in the figure and the height profile of Doppler velocity at AZ 180° in 2km distance which is the same as the figure. It also corresponds to the fact that Doppler velocity distribution in the high-level part of fog by horizontal scanning during the same time period caught the echo pattern moving from the south to the north as time passes. The above observation results prove that radar reflectivity factor and Doppler observation accurately grasp the status of ocean fog carried from the ocean to the ground by the current of high-level layer wind, which is the key to the study of fog movement.

#### 5. CONCLUSIONS

We examined the initial observation of Ka-band Doppler radar and confirmed it's potential as a reliable tool for cloud/fog observation. We made sure of the following three points:

- (1) Able to gain approx.  $\pm 40$ m/s of Doppler velocity including unfolding correction.
- (2) Able to observe the structure of multi-layer clouds.
- (3) Able to observe the structure of sea fog.

#### REFERENCES

- Kropfli R.A., Mastrosov S.Y., Uttal T., Orr B.W., Frish A.S., Clark K.A., Bartram B.W., Reinking R.F., Snider J.B., and Martner B.E., "Cloud physics studies with 8mm wavelength radar", Atmospheric Research, vol.35, pp.299-313,1995
- Pasqualucci F., "Drop size distribution measurements in convective storms with a vertically pointing 35GHz Doppler radar", Radio Science, vol.19, No.1, pp177-183, Jan.-Feb.1984
- Yanagisawa Z, Ishihara M. and Sawai T, Sea fog observation by a millimeter wave radar, Tenki,Vol.33, No.11, pp603-612, 1986 [In Japanese]

Table 1 Main specifications

Frequency	35GHz
Antenna Type	Cassegrain, 2m $\phi$
Antenna Gain	54dB
Beam Width	0.3°
Transmitter Tube	Magnetron
Peak Power	100kW
Duty	<0.0005
PRF(Double Pulse)	450/4500pps
Nyquist Velocity	$\pm 9.7$ m/s
Pulse Length	0.5 $\mu$ s
Dynamic Range	70dB(Log), 40dB(Lin)
Noise Figure	4dB
Polarization	Horizontal
Scan Range	AZ all direction
	EL -2° to +92°

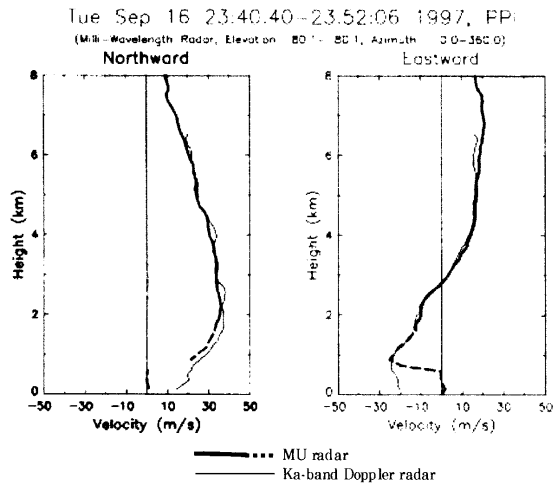


Figure 2 Comparison of the horizontal velocities observed by the MU radar and the Ka-band Doppler radar.

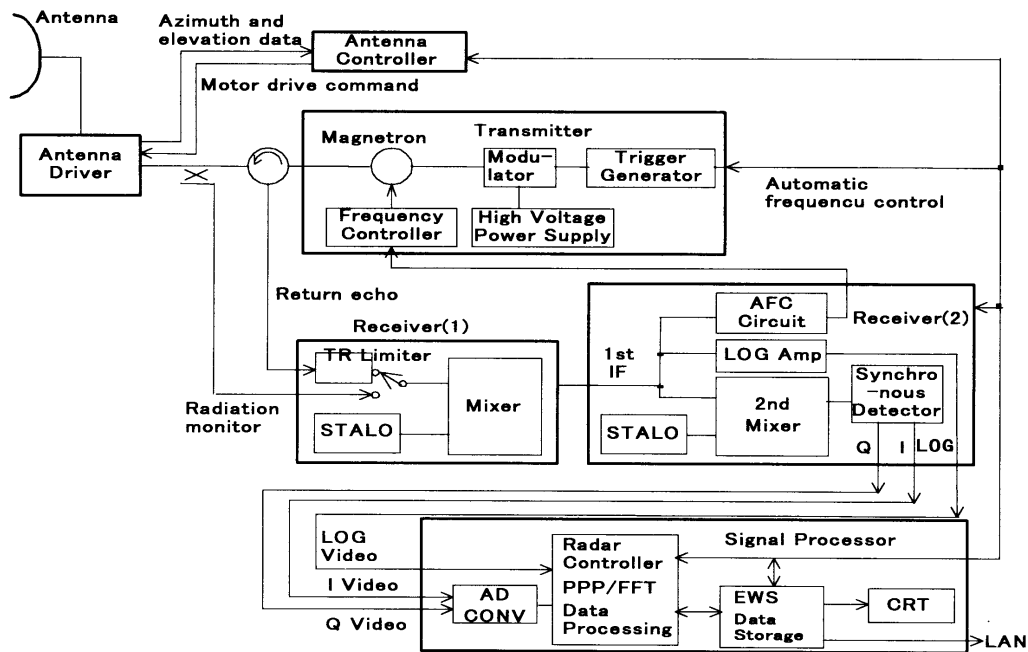


Figure 1 System Block diagram of the Ka-band Doppler radar.

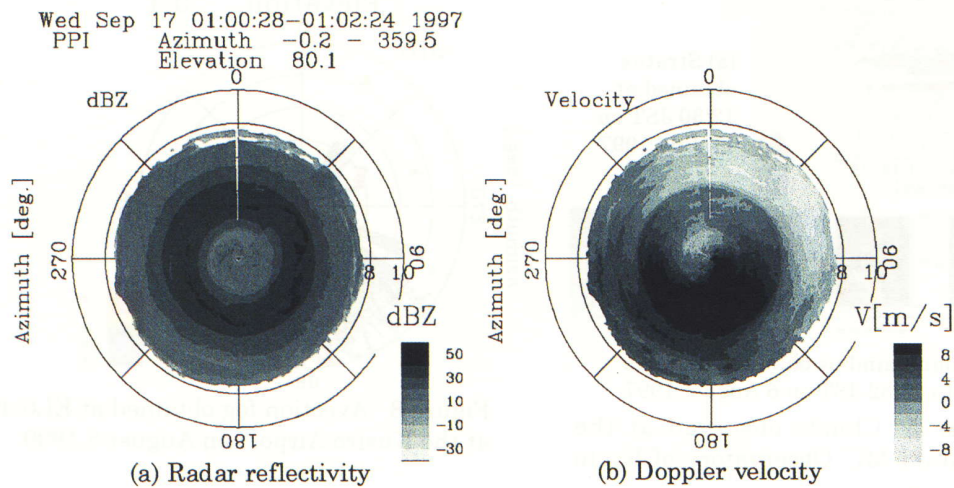


Figure 3 PPI observation of a stratiform cloud obtained at EL80° at the Sigaraki MU observatory of Kyoto University on 17 September 1997.

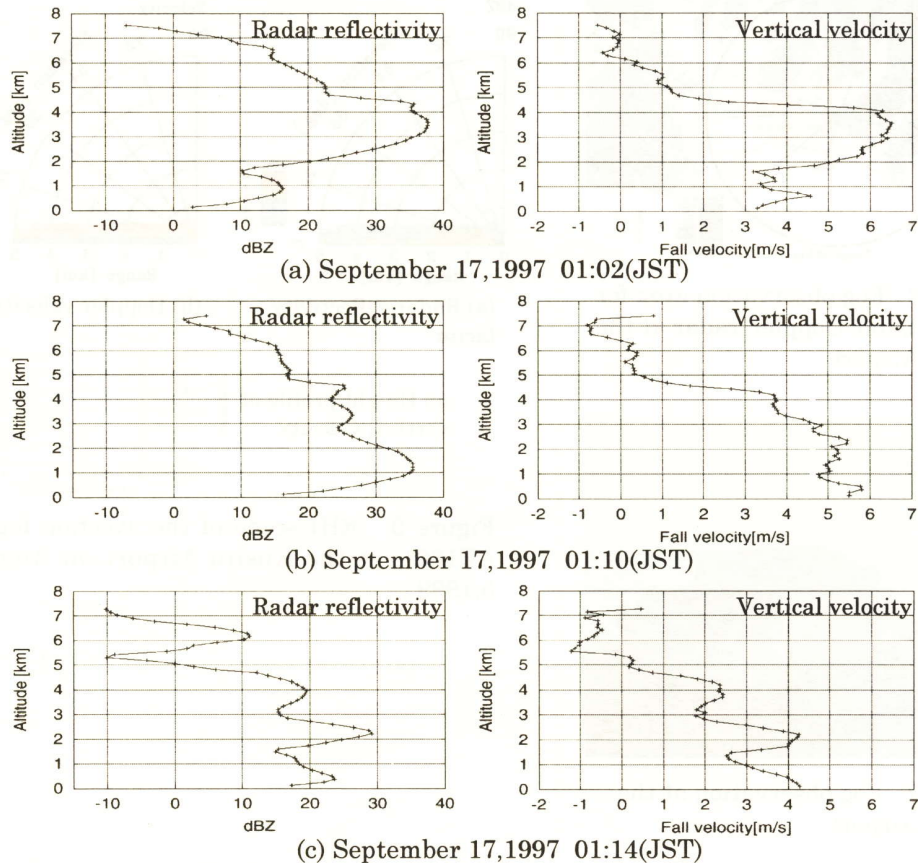
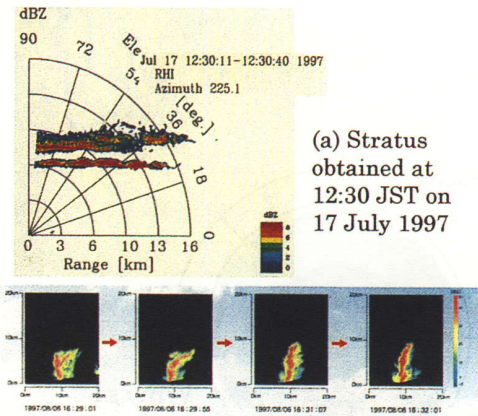


Figure 4 The profile of radar reflectivity and vertical velocity of a stratiform cloud obtained at the Sigaraki MU observatory of Kyoto University.



(a) Stratus obtained at 12:30 JST on 17 July 1997

(b) Cumulonimbus obtained between 16:29 to 16:32 JST on 6 August 1997

Figure 5 Clouds observed at the Shigaraki MU Observatory of Kyoto University.

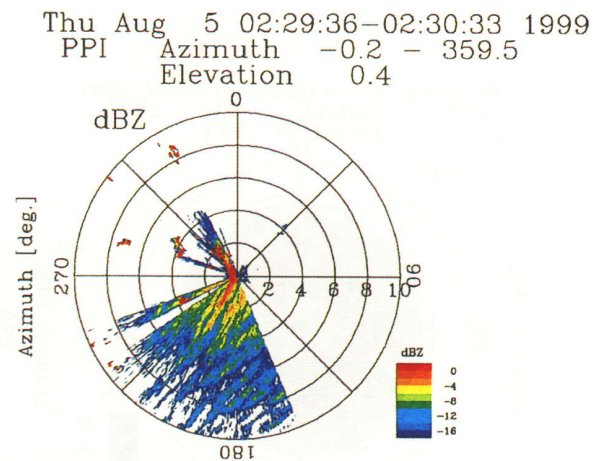


Figure 8 Avection fog obtained at EL0.4° at the Kusiro Airport on August 5, 1999.

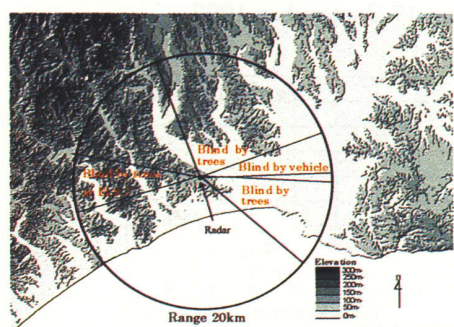
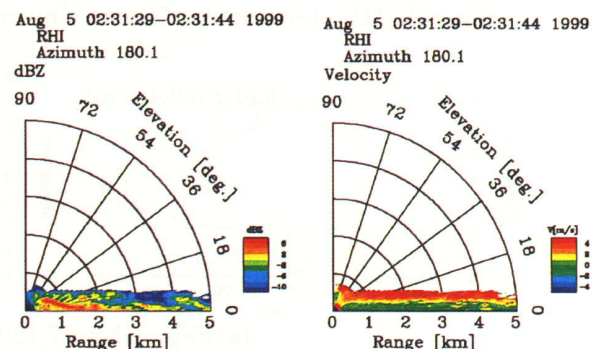
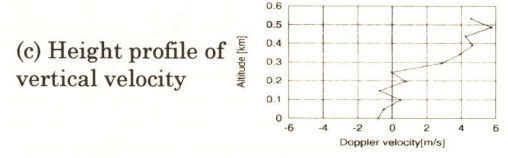


Figure 6 Fog observation area for the Ka-band Doppler radar at the Kusiro Airport



(a) Radar reflectivity factor

(b) Doppler velocity



(c) Height profile of vertical velocity

Figure 9 RHI scope of the avection fog at AZ180° at the Kusiro Airport on August 5, 1999.



Figure 7 Fog observation at the Kusiro Airport